The role of temperature in the formation of human–mimetic artificial cell membranes using droplet interface bilayers (DIBs)

Jaime L. Korner & Katherine S. Elvira

2021

The role of temperature in the formation of human-mimetic artificial cell membranes using droplet interface bilayers (DIBs)

Jaime L. Korner and Katherine S. Elvira*

Department of Chemistry, University of Victoria, Victoria, BC, Canada

E-mail: kelvira@uvic.ca

Abstract

Droplet interface bilayers (DIBs) have recently started to be used as human-mimetic artificial cell membranes. DIBs are bilayer sections created at the interface of two aqueous droplets, such that one droplet can be used as a donor compartment and the other as an acceptor compartment for the quantification of molecular transport across the artificial cell membrane. However, synthetic phospholipids are overwhelmingly used to create DIBs instead of naturally derived phospholipids, even though the diverse distribution of phospholipids in the latter is more biomimetic. We present the first systematic study of the role of temperature in DIB formation, which shows that the temperature at which DIBs are formed is a key parameter for the formation of DIBs using naturally derived phospholipids in a microfluidic platform. The phospholipids that are most abundant in mammalian cell membranes (phosphatidylcholine (PC), phosphatidylethanolamine (PE), phosphatidylserine (PS), and phosphatidylinositol (PI)) only form DIBs when the temperature is above the phase transition temperature (T_m). Similarly, DIB formation usually only occurs above the highest T_m of a single phospholipid in a bespoke formulation. We show a new phenomenon wherein the DIB "melts"

without disintegrating for bilayers formed predominantly of phospholipids that occupy cylindrical spaces. We also demonstrate differences in DIB formation rates as well as permeability of biomimetic membranes. Given the difficulties associated with making DIBs using naturally derived phospholipids, we anticipate this work will illuminate the role of phospholipid phase transition in mono- and bilayer formation and lay the foundation for DIBs to be used as human-mimetic artificial cell membranes.

Introduction

The use of microfluidic technologies to create artificial lipid bilayers provides advantages over more traditional methods, such as planar lipid bilayers[1] or those formed in bulk emulsions,[2] in terms of reproducibility, throughput, and control over the bilayer composition. In recent years, researchers have developed innovative microfluidic methods for the formation of model membranes, such as liposomes,[3] vesicles,[4] coacervates,[5] proteinosomes,[6] and supported planar bilayers.[7] We have recently shown that droplet interface bilayers (DIBs) are able to model cell membranes for the prediction of molecular transport *in vivo*.[8]

DIBs are formed when phospholipids are added to aqueous droplets in an oil phase (Video S1). A phospholipid monolayer spontaneously self-assembles at the oil-water interface. Then, when these coated droplets are brought into contact, a phospholipid bilayer forms at their interface such that the interfaces between two or more neighbouring droplets become biologically relevant artificial membranes. The first DIBs, made from the synthetic phospholipid 1,2-diphytanoyl-*sn*-glycero-3-phosphocholine (DPhPC), appeared in the literature in 2006.[9] In the years following, research groups around the world have created and used DIBs in a variety of different ways, such as to quantify molecular transport for drug discovery,[8,10] redto investigate water permeability,[11,12] to measure electrophysiological bilayer properties,[13–15] and to study the insertion of pore-forming proteins, mainly α-haemolysin.[9]

DIBs have been generated using microfluidic methods[16] and manually through the implementation of micromanipulators and electrodes.[13] In both cases, lipids can be added either

to the oil phase ("lipid-out"[9]) or the aqueous phase ("lipid-in"[17]). Since the first DIBs were created, they have predominantly been formed using the single synthetic phospholipids 1,2-dioleoyl-*sn*-glycero-3-phosphocholine (DOPC)[16,18,19] and DPhPC.[13,17,20–22] This is most likely due to the stability of droplet-coating monolayers formed using these phospholipids, which we attribute to the chemical structure of the phospholipids and their low phase transition temperatures (T_m). Based on robust archaeal phospholipids, DPhPC was designed and synthesized to have completely saturated acyl chains and an extremely low T_m.[23] Sparse publications exist demonstrating the use of single phospholipids that are more relevant to biological systems,[24–27] or of more complex mixtures, which are currently limited to non-human systems such as total lipid extracts from soy,[28] *E. coli*,[27] and porcine brain.[29]

However, to be fully usable as model artificial cells, DIBs need to mimic the salient features of human cell membranes. Mammalian plasma membranes are mainly comprised of the phospholipids phosphatidylcholine (PC), phosphatidylethanolamine (PE), phosphatidylserine (PS), and phosphatidylinositol (PI).[30–32] Other key components include cholesterol, sphingophospholipids (specifically sphingomyelin), glycolipids, and membrane proteins, including transporters.[32] The phospholipids present in cell membranes contain a distribution of tail lengths and degrees of saturation (Figure 2).[32] Thus, naturally derived phospholipids contain a single head group but a wide distribution of acyl chain lengths and saturation levels. Conversely, synthetic phospholipids such as DPhPC and DOPC contain only one head group and identical acyl chains throughout. To date, we have published the only example of DIBs made using naturally derived phospholipids found in human cell membranes (PC and PE),[8] incorporating more than one head group as well as many different acyl chain structures.

One of the main advantages of using DIBs as artificial cell membranes is that there is a donor and an acceptor compartment on either side of the artificial cell membrane. Hence, molecular transport across the membrane can be isolated and quantified. An additional functionality that DIBs provide is the ability to create bespoke lipid formulations to investigate the relationship between membrane composition and transcellular molecular transport. Our

focus here is to develop methods for the formation of biomimetic DIBs using phospholipid formulations made from naturally derived phospholipids containing many different acyl tails. In this paper, we define a "lipid formulation" as a customized mixture of naturally derived phospholipids at predetermined concentrations. We aim not to replace but to complement the use of total lipid extracts in the formation of DIBs. Total lipid extracts are perhaps more similar in some ways to the phospholipid composition of cell membranes, but also include many unknown components.[33] Therefore, the use of phospholipid formulations to make DIBs allows us to precisely study the effect of membrane composition on molecular transport and DIB formation rates.

We present here a systematic study of the role of temperature in DIB formation using naturally derived phospholipids and bespoke formulations. The role of temperature in DIB formation and stability has been investigated using total lipid extracts[27,29,34?,35] as well as single synthetic phospholipids.[36] Yanigasawa et al. found that following DIB formation, increasing the temperature led to droplet coalescence when using saturated phospholipids and no change when using unsaturated phospholipids. They used synthetic lipids. Work from the Sarles group has focused on manipulation of temperature prior to droplet contact, facilitating DIB formation using complex lipid mixtures.[27,29] They found that brain total lipid extract[29,34,35,37] and E.coli total lipid extract[27] both require heating to enable DIB formation rather than droplet coalescence.

We have performed an in-depth investigation of DIB formation for use as artificial cell membranes using a variety of mammalian phospholipids and phospholipid formulations, varying both head groups and acyl chain length and saturation. We designed a microfluidic platform to form these DIBs at biomimetic temperature and pH conditions. By controlling these properties, we can answer biophysical membrane questions more accurately than was previously possible. We are also able to form DIBs using complex phospholipid formulations, moving closer to the creation of truly biomimetic artificial cell membranes. Using the "lipid-in" approach, we made DIBs from the main phospholipids found in mammalian cells (PE,

PC, PS and PI) and of different ratios of each of these lipids to create bespoke formulations for DIB formation. The "lipid-in" approach was selected due to previous data demonstrating the role of phase transition temperature in monolayer assembly at a phase interface.[38] All phospholipids used are naturally derived, meaning that only one head group but a distribution of acyl chain lengths and saturation is present in each sample. We also demonstrate DIB formation using formulations of these phospholipids. The main difficulty with making DIBs from phospholipid formulations is the fact that each single phospholipid present may have a different T_m. Our data show that varying and controlling the temperature of the microfluidic device allows for successful DIB formation at or above the phospholipid T_m values, even for complex phospholipid formulations. Using bilayers formed from selected phospholipid formulations, we also demonstrate differences in the fluorescein transport flux as well as rate of bilayer formation.

Results and discussion

We designed our microfluidic device for DIB formation (Figure 1) to enable a high level of control over droplet position on the chip, droplet volume, and droplet speed and hence the speed at which droplets come together to form a DIB. As described previously,[8,39] DIB formation requires that droplets are brought into contact with each other slowly, especially when compared to the speed at which droplets are usually formed in microfluidic devices.[40] There are two reasons for this. Firstly, there must be enough time between droplet and DIB formation on the chip to allow the phospholipids to form a complete (hole-free) monolayer at the droplet surface, otherwise droplets will coalesce when they come into contact with each other (Video S2). Our droplets were brought together at an approximate velocity of $200\,\mu m\,s^{-1}$, which corresponds to a Reynolds number of 0.00143. When forming DIBs on microfluidic devices, the fluid dynamics and channel effects on the microscale yield faster monolayer formation times using the "lipid-out" method than "lipid-in," as opposed to non-

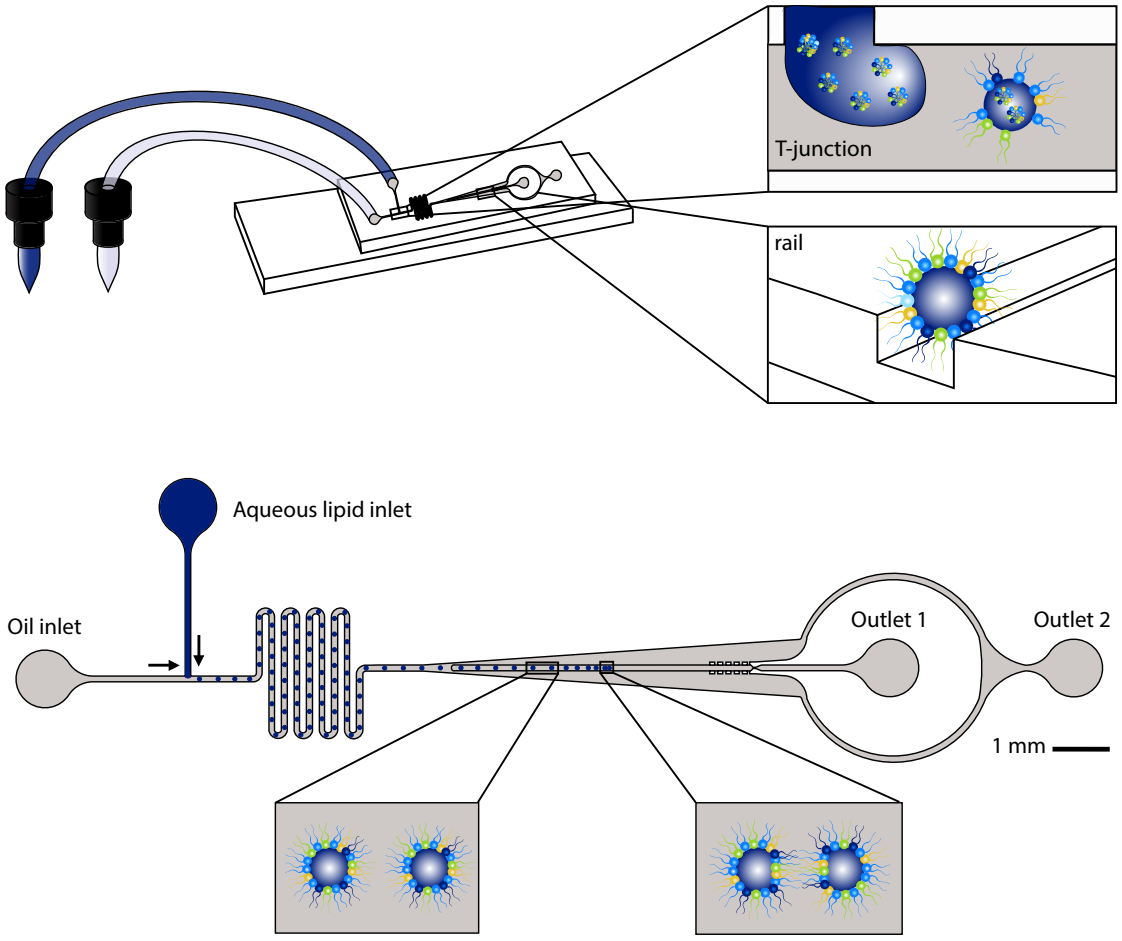

Figure 1: **Design of the microfluidic platform for DIB formation.** Top: 3D depiction of the microfluidic device and experimental setup. Droplet formation occurs at the T-junction (see inset), where the squalene (grey) and aqueous (blue) streams meet. The aqueous phase, containing phospholipid vesicles, forms droplets in the bulk oil phase and monolayer self-assembly begins. A widening chamber is used to slow down the droplets so that the aqueous droplet is completely coated by a phospholipid monolayer and is guided down the centre of the chamber by a rail (see inset). Bottom: Top-down view of the design of the microfluidic device. The microfluidic device is drawn to scale. The insets represent phospholipid-coated droplets just before contact and droplets after DIB formation. In our microfluidic device, these droplets have a diameter of around 100 µm. Phospholipids are not drawn to scale to show their arrangement in a DIB.

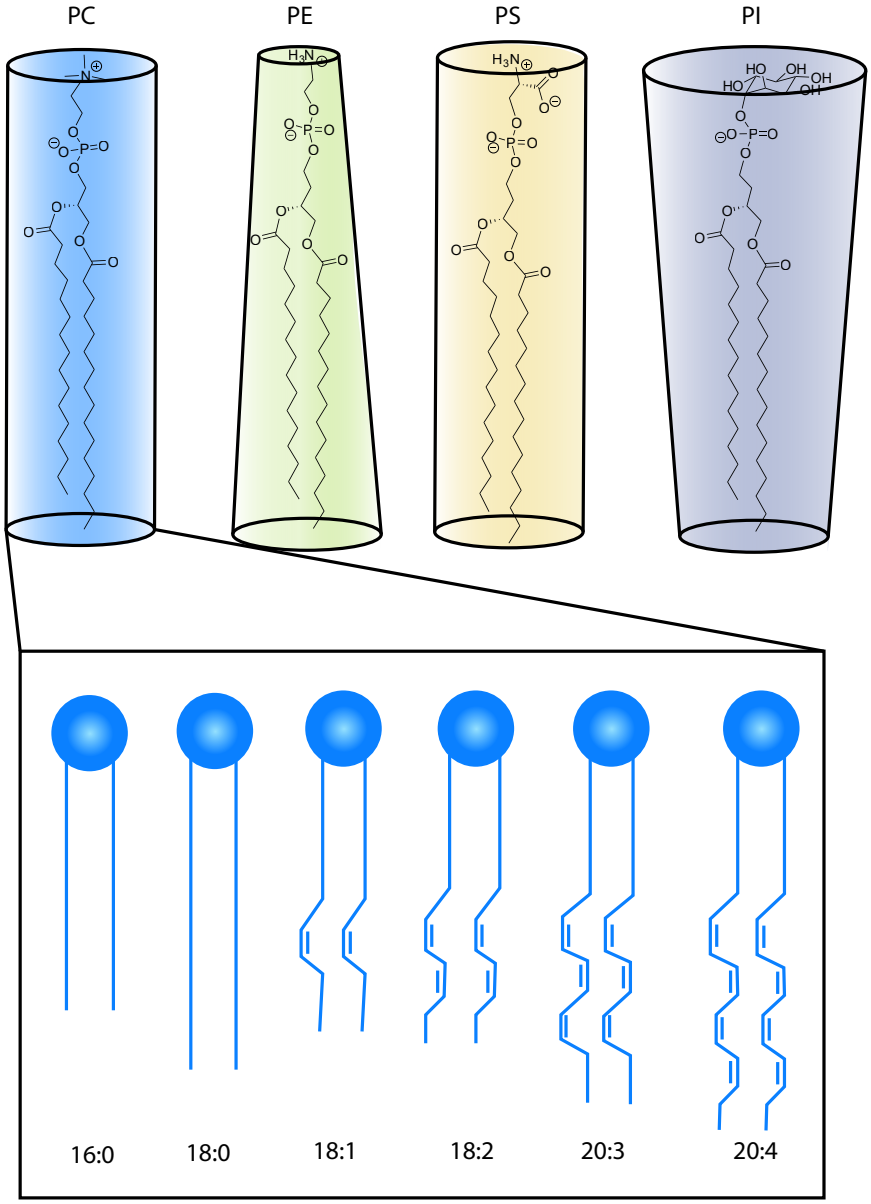

Figure 2: **Shapes and compositions of naturally derived phospholipids.** Top: From left to right, the structures of 16:0 PC, PE, PS, and PI are shown in the three-dimensional shapes they occupy. PC and PS are cylindrical, while PE is inverted conical and PI is conical. Bottom: While all the lipids in naturally derived Liver PC have a choline head group, multiple acyl chains are present. These tail groups are illustrated here, highlighting the difference lengths and degrees of unsaturation.

microfluidic DIB formation.[41] Off-chip, monolayer formation times are close to 5 minutes for the "lipid-in" method and up to 30 minutes for "lipid-out."[42] Secondly, even when droplets are fully covered with a phospholipid monolayer, the speed at which they are brought into contact with each other must be slow enough to enable a bilayer to form between the droplets. Ideal droplet velocity and lipid concentration for DIB formation have previously been investigated.[39] Once a bilayer is formed while the pressure pump is off, turning the pressure pump back on does not cause droplet coalescence. If a DIB forms under flow conditions, the oil flow around the DIB pair does not cause the bilayer to rupture. However, prior to full bilayer formation, the interface between the droplets is delicate and hence susceptible to droplet merging since there are no other stabilising molecules in the system. Prior work has shown that droplets must be brought together at low velocities to form a DIB and avoid droplet coalescence.[39] Here, so long as the device was held at the appropriate temperature, droplets can be brought together quickly and under flow conditions, demonstrating the effectiveness of the phospholipids as a surfactant. Droplet velocity at the point of contact appears to be a secondary factor in determining the success of DIB formation: when velocity, phospholipid concentration, and microfluidic device design are constant, change in temperature appears to dictate DIB formation success. Therefore, to be able to determine whether it is possible to form DIBs using phospholipids found in human cell membranes, we designed the microfluidic device such that the forces that the device subjects the droplets to was not an experimental variable.

Aqueous suspensions of each phospholipid or phospholipid formulation are prepared in a buffer and inserted into the microfluidic device using a pressure pump. Simultaneously, squalene is pumped into the device through a perpendicular channel at a similar pressure, so that aqueous droplets form at the T-shaped junction where the two channels (and thus the aqueous and oil streams) meet (Figure 1). After budding off at this intersection, the aqueous droplets become coated with a phospholipid monolayer as the vesicles inside the droplets contact the oil-water interface. To allow enough time for this process to occur without

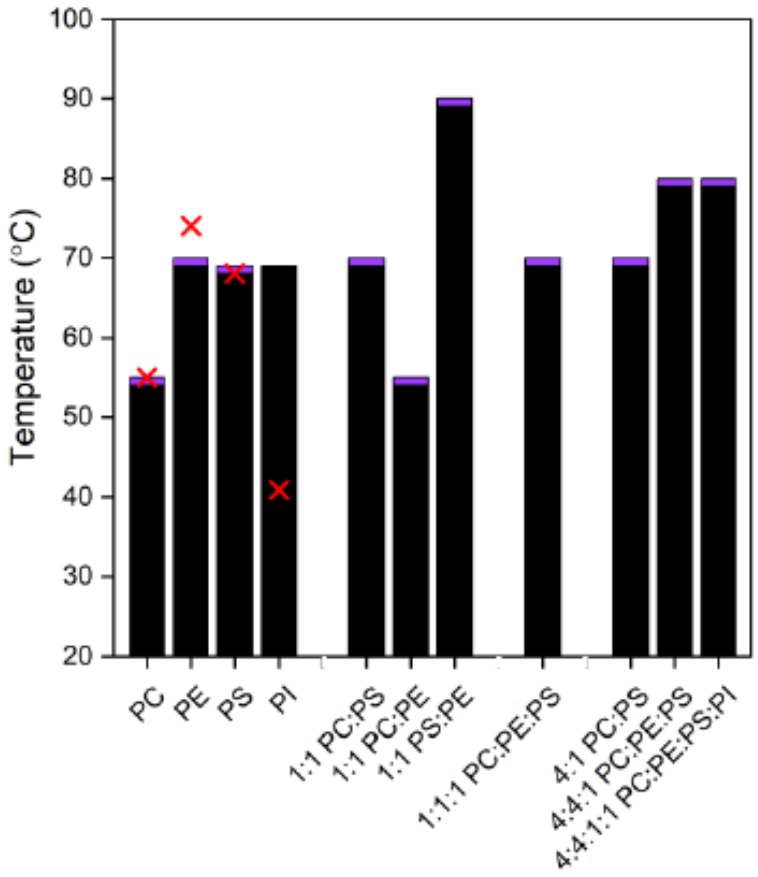

Figure 3: **Temperatures at which DIB formation occurs with different phospholipids.** We tested DIB formation of four naturally derived phospholipids and phospholipid formulations over a range of temperatures, beginning at ambient temperature (20°C). Black indicates that DIB formation was not possible (droplets merged upon contact) and purple indicates successful DIB formation. At constant pressures and lipid concentrations, DIB formation consistently failed below the indicated temperature and consistently occurred above the indicated temperature. Red crosses indicate the T_m of the dominant component of each natural phospholipid. In the phospholipid formulations, the biological source of PC, PE and PI is liver, and that of PS is brain.

significantly increasing device size, a meandering channel section immediately follows the droplet formation junction. After exiting the meander, phospholipid-coated droplets enter a gradually widening chamber, which causes a decrease in the speed of the droplets since an equal volume of fluid is now present in a larger chamber. This chamber also has a second layer which consists of a "rail" etched into the chamber that guides the droplets on a straight path down its centre.[43] Droplets can be stopped precisely anywhere in the device using the pressure pump, as we did when gathering the data shown here (Video S3). Stopping the pressure pump stops the droplets in place,[8] and DIB formation occurred as they flowed down the rail. The microfluidic device was designed for use in any lab, even without access to expensive pressure pumps. Formation of DIBs on the rail has its own advantages, as the use of pillars in droplet traps, another method for DIB formation, is linked to increased droplet merging.[44] As the fluid flow rate slows in the chamber and the droplets are guided by the central rail, the droplets come into contact and a DIB forms at each point of contact. Successful DIB formation is defined as lack of droplet merging and formation of a distinctive and visible bilayer section at the interface (Figure 4a).

Since amphiphilic lipids will spontaneously form large, multilamellar vesicles in aqueous solution,[45] prior to introduction into the microfluidic device, phospholipid suspensions were first extruded through a porous membrane to create small, unilamellar vesicles. In this work, we use the "lipid-in" approach for DIB formation. Using our microfluidic platform, we first tested DIB formation using each of these phospholipids (PC, PS, PE and PI) separately, and then tested various phospholipid formulations over a range of temperatures both above and below the T_m of each phospholipid or phospholipid formulation. We held the pH of the aqueous lipid suspensions constant to account for any potential differences in T_m that can arise with changes in phospholipid protonation state.[46] We designed binary, ternary, and quaternary phospholipid formulations to mimic the ratios in which these phospholipids are found in mammalian cells[47] and have previously been used to model molecular transport in cell-mimetic systems.[48] We used naturally derived phospholipids to ensure that our DIBs are

made from phospholipids that contain the diverse distribution of acyl chains found *in vivo.*

T_m values are rarely determined for naturally derived phospholipids, but can be found for some of their components. In fact, T_m values for naturally derived lipids and lipid extracts are not reported by lipid suppliers or in the literature. To estimate the T_m of a naturally derived lipid, which contains a distribution of acyl chains, suppliers recommend using the T_m of the predominant lipid component. For example, no T_m value is reported for Liver PC as a whole, but the major component of Liver PC (18:0 PC[49]) has a T_m value of 55°C.[50] We approximate T_m values for each of the naturally derived phospholipids from the major component of each. Similarly, since there are no literature T_m values for our bespoke phospholipid formulations, we determined experimentally a range of temperatures at which DIB formation was possible for each phospholipid formulation (Figure 3). Droplets were formed in high throughput, at an approximate rate of one droplet per second and DIB formation was observed over the course of a minute for each condition. A custom-made heating platform,[8] was used to accurately control the temperature in the microfluidic device and hence the temperature of DIB formation. The heating platform setpoints were increased from room temperature and droplet behavior (coalescence or DIB formation) was observed (Table S1). Data was collected during temperature ramp-up as well as at each setpoint, allowing us to test the effects of every temperature point on DIB formation. We tested each naturally derived phospholipid or phospholipid formulation on 2-4 different microfluidic devices.

As mentioned previously, naturally derived phospholipids containing more than one acyl chain type are not usually used to form DIBs. This is likely due to the instability of the phospholipid monolayer (and hence high occurrence of droplet merging) at room temperature, which is significantly below the T_m of these phospholipids. We know that failure to form a DIB due to droplet merging can happen if droplet velocity at the time of attempted contact is too high[39] or if phospholipid monolayer formation is incomplete.[27] Additionally, a full monolayer will not form if the concentration of phospholipid is too low.[39] Our data show (Figure 3) that DIB formation also does not occur if the temperature of the microfluidic

channel is below the T_m of the phospholipids for single phospholipids. We observed successful DIB formation using Liver PC, Egg PC, Liver PE, and Brain PS near or above the T_m of the major component of each (Figure 3, Table S1).

Liver PI alone did not form DIBs under any experimental conditions, likely due to its shape and corresponding low packing parameter. PI is an inverted conical phospholipid, meaning that the head group is significantly larger than the tail groups, disallowing the assembly of tightly packed monolayers and bilayers on the curved surfaces of droplets[32,51–54](Figure 2). We also tested DIB formation using formulations of the mentioned naturally derived phospholipids (Figure 3). The binary formulations of PC and PS (in both 1:1 and 4:1 ratios) formed DIBs at 70°C and above, which aligns with the T_m of PS at 68°C.[50] As expected, we found that a ternary formulation of PC, PE, and PS (4:4:1) successfully formed DIBs at and above 80°C. Surprisingly, adding PI to create a quaternary formulation (4:4:1:1 PC:PE:PS:PI) did not prevent DIB formation, indicating that the mono- and bilayer stabilizing effects of the other three phospholipids were dominant. We propose that the curvature of the droplet and the membrane surface plays a larger role when using PI alone versus as a minor component of a formulation. These data appear to agree with the literature showing phases with the opposite curvature when using inverted conical surfactant molecules.[32,51–54]

Also interesting is the fact that 1:1 PC:PE formed DIBs at 55°C and above, which falls between the T_m values of the two formulation constituents. This behavior is only observed when using the "lipid-in" approach; we have previously demonstrated "lipid-out" DIB formation using 1:1 PC:PE at physiological temperatures (37°C).[8] We propose that the increased energy input needed to facilitate monolayer formation using the "lipid-in" approach is due to the difference in phospholipid structure formation in the aqueous and oil phases. Phospholipids extruded into an aqueous phase form uniformly sized unilamellar vesicles, which exist in a gel phase as long as they are held below the appropriate T_m. Heating the suspension to or above the T_m initiates a gel-to-liquid phase transition, which encourages

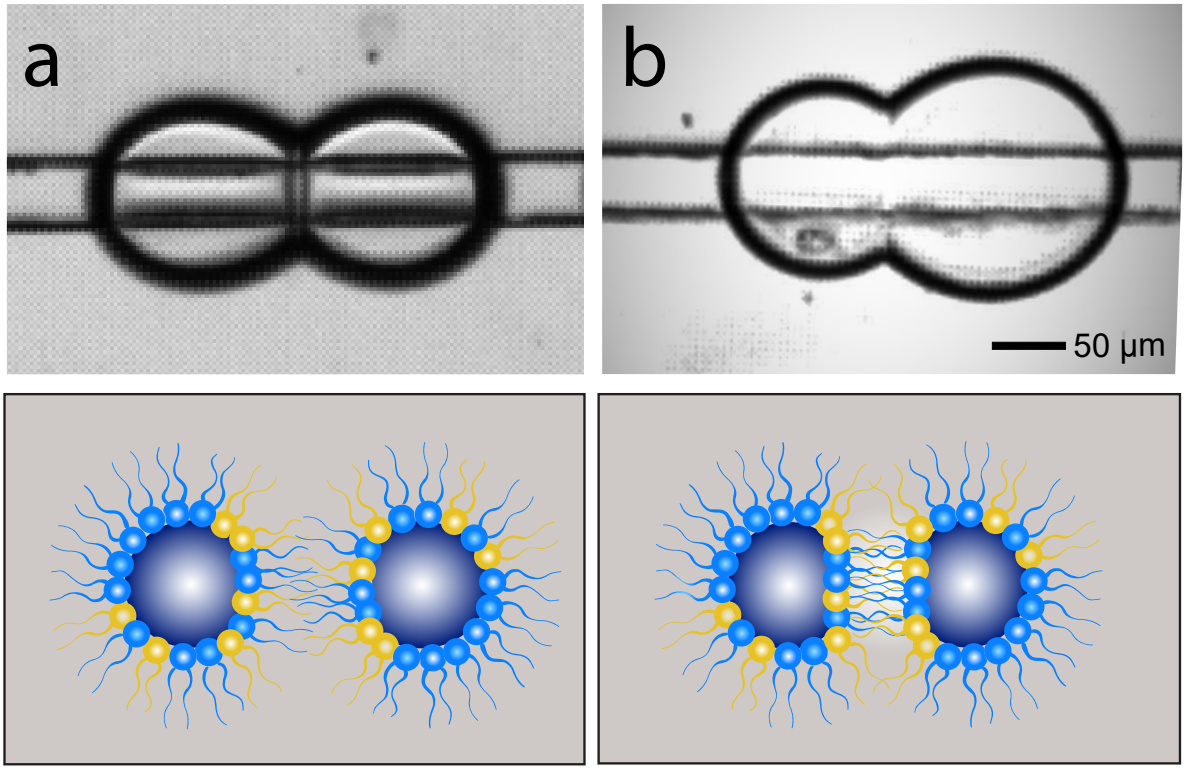

Figure 4: **"Melting" of the DIB bilayer over time.** DIB "melting" was observed when Egg PC, DPhPC, 1:1 PC:PS, and 4:1 PC:PS (cylindrical phospholipids) were used for DIB formation (Figure S1, Videos S4 and S5). a) Microscopy image showing DIB formation using 4:4:1 PC:PE:PS occurring when the droplets are brought in contact with each other. The schematic shows the bilayer formed between the droplets. b) Microscopy image showing that, at elevated temperatures, the "melty" DIB, here formed using 4:1 PC:PS, is extremely thin and nearly invisible. The schematic represents a more efficient packing of the lipid tails. The scale bar is 50 µm in all microscopy images. Phospholipids are not drawn to scale.

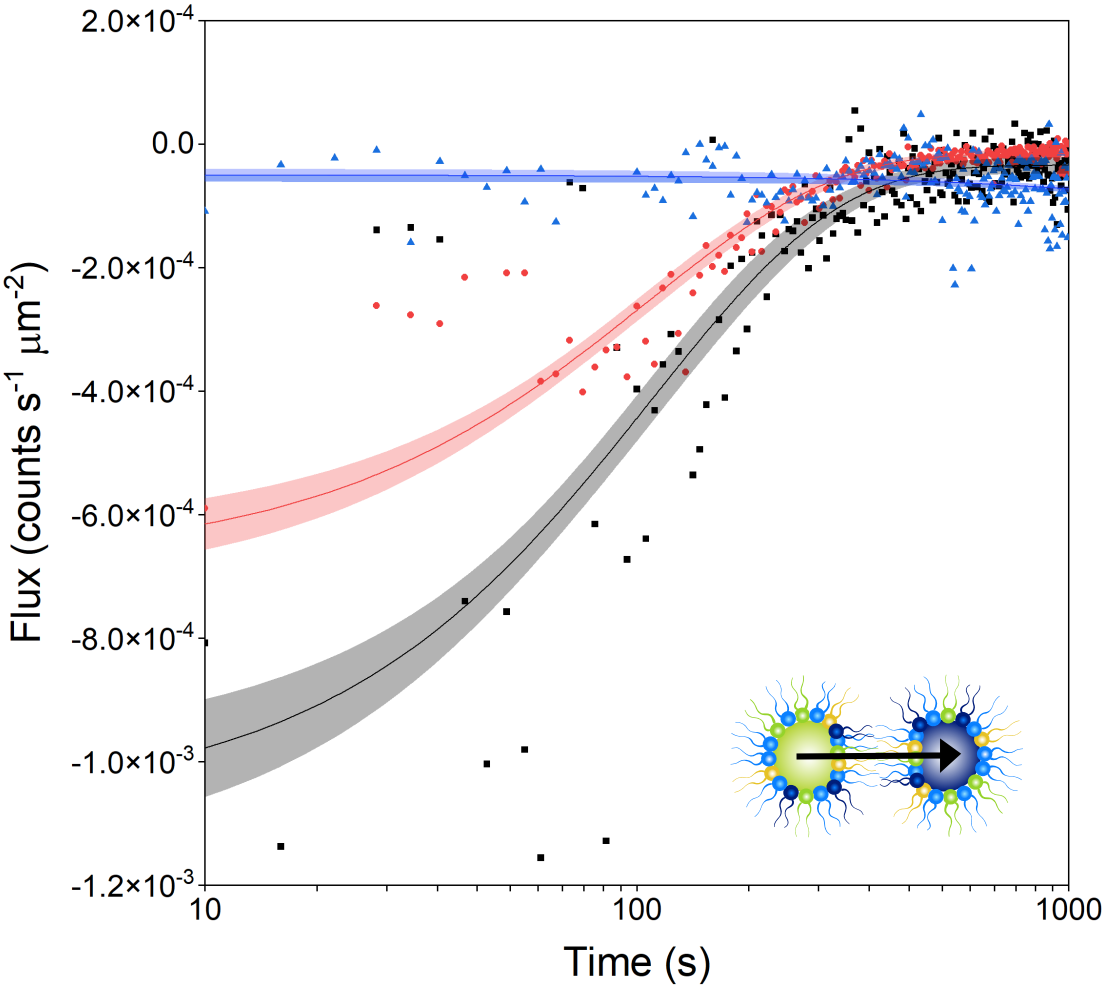

Figure 5: **Fluorophore flux over time in three different lipid formulations.** Following DIB formation between a donor (containing fluorophore) and an acceptor (empty) droplet, diffusion of fluorophore through the bilayer was measured, as shown in the diagram in the inset. Data shown for the flux of fluorophore across bilayers formed using 4:1 PC:PS (black), 4:4:1 PC:PE:PS (red), and 4:4:1:1 PC:PE:PS:PI (blue). Maximum flux and fluorophore half-life were determined using the fitted curve and are shown in Table 1. The microfluidic device was held at 37°C while fluorescein transport occurred. An exponential curve was fitted to these data and 95% confidence bands were calculated from the standard deviation at each timepoint in OriginPro.

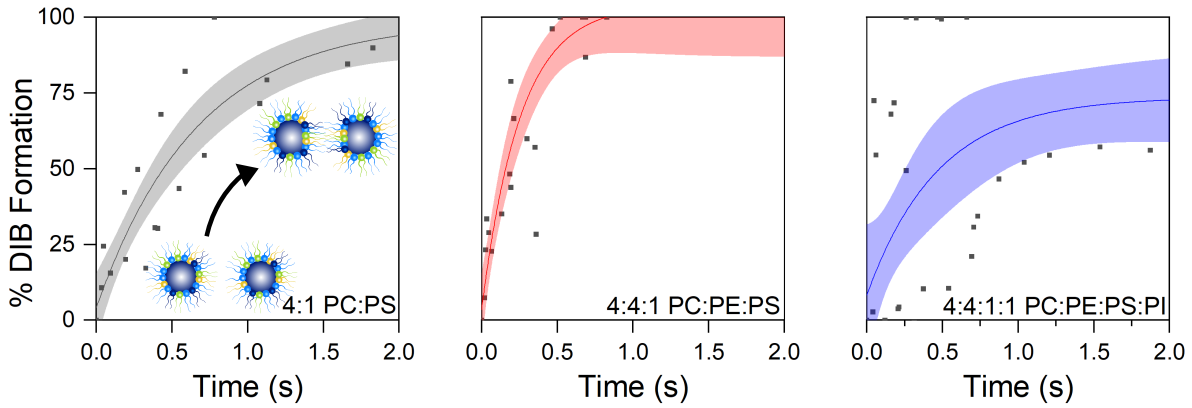

Figure 6: **Ratio of DIB diameter to droplet circumference.** To assess differences in the rate of DIB formation, we measured the ratio of DIB diameter to droplet circumference of 4:1 PC:PS (black), 4:4:1 PC:PE:PS (red), and 4:4:1:1 PC:PE:PS:PI (blue) and normalized these data as a percentage. A DIB formation value of 0% indicates complete droplet separation and lack of DIB formation. As a DIB forms, more of the droplet circumference is involved in bilayer formation and the DIB formation approaches 100% (see inset in first graph). An exponential curve was fitted to these data and 95% confidence bands were calculated from the standard deviation at each timepoint.

monolayer formation. On the other hand, phospholipids are soluble in oil and so do not require a higher temperature to self-assemble at the droplet-oil interface of the droplets to form a monolayer or a DIB.

To ensure that DIB formation is not affected by other components of the microfluidic platform, we tested other parameters that can potentially affect lipid distribution in DIBs. As previously discussed, droplet velocity at point of contact is a significant factor in successful DIB formation.[39] We applied pressures as low as 20 mbar to both the aqueous and oil channels, slowing droplets as much as possible while keeping droplet formation consistent. This did not result in successful DIB formation at room temperature for any of the phospholipids or phospholipid formulations shown in Figure 3. We also varied the composition of the oil phase, replacing squalene with hexadecane, which is more commonly used for DIB formation,[55] and observed no effect on the success of DIB formation. Finally, Najem et al. also found that extrusion of lipid suspension at elevated temperature encouraged easier extrusion.[34] However, we extruded the phospholipid suspensions at their T_m value rather

than at room temperature, but this again had no effect on the success of DIB formation. Hence, taking into account the relevant T_m values is key to successful DIB formation when using a "lipid-in" approach as it encourages complete formation of the droplet-coating phospholipid monolayer. This fits with prior work showing a correlation between temperature and completeness of the droplet monolayer covering, and hence successful DIB formation, using a total lipid extract from *E. Coli.*[27]

We also observe a new phenomenon where DIBs "melt" (Figure 4b). Given sufficient heat, the bilayers in these cases become extremely thin and nearly invisible, but the droplets do not merge. "Meltiness," which we define as the formation of a thin, nearly invisible bilayer, as shown in Figure 4b, occurs on the same timescale as "non-melty" DIB formation and does not reverse with a decrease in temperature. Using squalene as the oil mobile phase, we noticed DIB "melting" at 40°C and above for DPhPC (Figure S1, Video S5), 55°C and above for Egg PC (Table S1), 69°C for PS, and 70°C and above for both 1:1 and 4:1 PC:PS. Notably, Liver PC on its own did not melt; the presence of PS in a formulation appears to dictate both the T_m of the natural phospholipid formulation and whether melting occurs. DIB melting appears to occur at temperatures above the T_m in bilayers comprised of cylindrical phospholipids, i.e. DPhPC, PC, PS, and formulations thereof (Videos S4 and S5). This is likely a reflection of a more complete gel-to-liquid phase transition and thus higher ability of the phospholipids to pack together tightly. This phenomenon occurs with cylindrical phospholipids due to their ability to pack tightly together in a planar bilayer. The composition of phospholipid formulations appears to be a key factor in DIB thickness as "meltiness" was only observed using cylindrical phospholipids. Oil exclusion is unlikely to contribute to DIB "melting" because squalene is easily excluded from lipid bilayers[34,56] The "meltiness" could potentially be due to lipid exchange between leaflets or between the monolayer and bilayer sections; this will be a focus of future work.

We then selected three phospholipid formulations to investigate whether lipid composition affects the passive molecular transport of fluorescein. We tested 4:1 PC:PS, 4:4:1 PC:PE:PS,

and 4:4:1:1 PC:PE:PS:PI. Initial transport rates were highest in the binary phospholipid formulations and decreased as the formulation complexity increased (Figure 5). Increasing membrane permeability has previously been found to correlate with a decreasing proportion of PC in the model membrane.[24] Following curve fitting, we determined the y-intercept, j_{max}, as well as the fluorophore half-life for all three formulations (Table 1). Although the maximum flux differs by an order of magnitude between each of the three phospholipid formulations, the fluorescein half-life for the binary and ternary phospholipid formulations is essentially identical. This indicates that bilayer phospholipid composition affects initial rates of fluorescein transport, but those rates equilibrate to give similar half-lives.

Bilayer packing depends on membrane lateral pressure and phospholipid type.[24] The relative lateral pressure of a leaflet of the bilayer, π, can be determined using the equation $\pi = \gamma(1 - cos\theta)$, where γ is the interfacial tension of the monolayer and θ is the half contact angle between the droplets comprising the DIB.[24] We measured γ and θ for these bespoke lipid formulations and calculated π for each (Table S2). For 4:1 PC:PS, 4:4:1 PC:PE:PS, and 4:4:1:1 PC:PE:PS:PI, the lateral pressure was found to be, respectively, (2.35 ± 0.05) mN/m, (3.92 ± 0.86) mN/m, and (4.13 ± 0.23) mN/m. This demonstrates the significant effect membrane composition has on lateral pressure and packing. Membranes formed using only cylindrical phospholipids demonstrate the lowest lateral pressure. Addition of the conical lipid PE as well as the inverted conical lipid PI correlate with an increase in lateral pressure. This trend aligns with the observed permeability trend: more tightly packed membranes are less permeable, as observed using DIBs formed using 4:4:1:1 PC:PE:PS:PI. This correlation between lateral pressure and permeability has been previously observed[24] in DIBs formed using synthetic phospholipids.

In addition to the observed permeability effects, we hypothesized that changing the phospholipid formulation would alter the rate of DIB formation. We propose that the size, shape, and charge of the phospholipids included in the formulation influences DIB formation rate. Bilayer formation depends on factors such as the viscosity of the oil phase, which must be

excluded from the bilayer region, and the energy of adhesion between droplets.[57,58] Bilayer formation also requires formation of a stable monolayer, which is encouraged by bringing the system to or above its T_m. We propose that monolayer formation is affected by the phospholipid head groups present and bilayer formation rate is affected by the tail groups. For the same three phospholipid formulations, 4:1 PC:PS, 4:4:1 PC:PE:PS, and 4:4:1:1 PC:PE:PS:PI, we measured the droplet circumference and DIB diameter over time above the T_m value for each phospholipid formulation for consistency, at 70°C, 89°C, and 84°C, respectively. Relative bilayer diameters were measured as a proxy for energy of adhesion. The DIB diameter was then divided by the droplet circumference for each droplet pair to give a ratio of DIB to droplet size. These measurements were performed on 3-5 DIB-connected droplet pairs for each lipid formulation. To account for minor variations in droplet size between replicates, these ratios were then normalized on a 0-100 scale (Equation S1). A value of 0% indicates that the droplets are completely separated and a value of 100% indicates that DIB formation is complete and the ratio of DIB diameter to droplet circumference is no longer changing. Data normalization details are provided in the ESI (Equation S1). The resulting values are plotted over time in Figure 6. Similar measurements were performed for videos in which DIBs "melted," but no significant difference was observed between the values or DIB formation rate between "melty" and non-"melty" DIBs. Lipid behavior differs between phospholipid formulations, giving DIB formation rates that depend on formulation when other variables, such as flow rate and identity of the mobile oil phase, are kept constant. Following curve fitting, we graphically determined $t_{1/2}$ values for DIB formation, which are given in Table 1. The highest rate of DIB formation, corresponding to the shortest half-life, was observed using the ternary mixture, followed by the binary and the quaternary mixtures. The complexity of phospholipid behavior means that no simple, linear relationship exists between the number of phospholipids in a mixture and the rate of DIB formation. Addition of the conical lipid PE to the binary mixture of cylindrical phospholipids PC and PS shortens DIB formation time significantly, potentially due to hydrogen bonding between the small,

charged amine head group of the PE and the phosphate groups on adjacent phospholipids.[46] However, incorporation of the inverted conical lipid PI in the quaternary mixture reduces the DIB formation rate again, indicating that the steric effect of the large inositol head group significantly influences lipid packing kinetics. It has been suggested that the use of squalene masks some of the effects of phospholipid type on DIB permeability, so it is possible that these effects may appear even more significant with use of a different mobile phase.

Table 1: **Quantifying the effect of membrane formulation on molecular permeability.** Maximum fluorophore flux (j_{max}), fluorophore half-life ($t_{1/2}$) and the time taken for bilayer formation (formation $t_{1/2}$) were determined for three bespoke phospholipid formulations. We measured fluorescence intensity over time in both the acceptor and donor droplets and show here the flux of fluorophore out of the donor droplet normalized for droplet volume and DIB surface area. Maximum flux and $t_{1/2}$ were determined graphically. The microfluidic device was held at physiological temperature (37°C) while fluorescein transport was observed and image data collected. To quantify DIB formation time, DIB diameter and droplet circumference were measured and the ratio of the two normalized as a percentage, as shown in Figure 6. DIB formation $t_{1/2}$ was determined graphically, indicating the timepoint at which the bilayer is halfway complete. Measurements were performed above the T_m for each phospholipid formulation.

Phospholipid	$\mathbf{j_{max}}$ **(counts** μ**m** $^{-2}$ **s**$^{-1}$**)**	$\mathbf{t_{1/2}}$ **(s)**	**Formation** $\mathbf{t_{1/2}}$ **(s)**
4:1 PC:PS	$-1.04 \times 10^{-3} \pm 4.824 \times 10^{-5}$	107.9±7.8	0.67±0.13
4:4:1 PC:PE:PS	$-6.60 \times 10^{-4} \pm 2.544 \times 10^{-5}$	104.7±5.8	0.26±0.06
4:4:1:1 PC:PE:PS:PI	$-5.03 \times 10^{-5} \pm 5.339 \times 10^{-6}$	N/A	0.47±0.24

Conclusions

We have developed a microfluidic platform that allows us to quantify the parameters associated with the formation of DIBs using naturally derived phospholipids (PE, PC, PS and PI) and bespoke formulations thereof for use as artificial cell models. We used phospholipids derived from mammalian biological sources to ensure that each phospholipid contained one type of head group and a distribution of acyl chain lengths and saturation levels, as occurs in cells. This is the first time that DIBs have been made using naturally derived phospholipids using the "lipid-in" approach, where lipids are dosed in the aqueous phase.

Our data show that to form DIBs in this way, droplets must be brought into contact with each other while they are at a temperature above the T_m of the phospholipid. For phospholipid formulations, the temperature must usually be above the highest T_m, though there is an interplay between T_m and the phospholipid shape, and hence packing ability. For example, PI, an inverted conical lipid, does not form DIBs alone at any of the temperatures tested, but does form DIBs when it is a minor component of a phospholipid formulation. We also show a new phenomenon in the field of DIB research. Over time, DIBs made from cylindrical phospholipids "melt" together without merging. We propose that this shows a more complete gel-to-liquid phase transition and formation of a more tightly packed phospholipid monolayer. We also show how molecular transport through the bilayer depends on the lipid formulation using fluorescein. Finally, we quantify how the lipid formulations affect the rate of formation of the DIB.

Since their first use, DIBs have been formed mostly using synthetic phospholipids such as DPhPC, and have predominantly been used to study passive or active (through pores such as α-haemolysin) molecular transport. However, as we have previously shown,[8] DIBs have the potential to be used as human-mimetic artificial cell membranes for drug discovery applications. Up until now, it has been experimentally complicated to form DIBs in a microfluidic device using naturally derived phospholipids, especially using the "lipid-in" approach. Our work shows that careful regulation of temperature allows DIB formation from the major components of mammalian cells. DIB "meltiness", the dependence of DIB formation rates on phospholipid formulation, and other biophysical lipid questions are interesting topics for further investigation. For example, by performing systematic studies correlating temperature, DIB formation rate, and DIB "meltiness" with lipid head and tail groups, employing single synthetic phospholipids to allow for a higher level of control. It would also be interesting to further investigate the potential effects of the oil phase composition on DIB formation and "meltiness". Impactful information on the biomimetic nature of DIBs will be gained if lipid domains can be shown to form in these systems, as well as through the

quantification of lipid exchange between monolayers. We look forward to seeing DIBs reach their full potential as artificial cell models by providing methods for DIB formation that allow the use of many more, and much more biologically relevant, types of phospholipids.

Materials and methods

Materials

All reagents were purchased from Millipore Sigma unless otherwise stated. Phospholipids were purchased from Avanti Polar Lipids. The biological sources of L-α-phosphatidylcholine (>99%) were egg and bovine liver. The biological source of L-α-phosphatidylethanolamine (>97%) and L-α-phosphatidylinositol (>99%) was bovine liver. The biological source of L-α-phosphatidylserine (>99%) was bovine brain. Reagents were purchased at the following grades: squalene (>98%), 4-(2-hydroxyethyl)-1-piperazineethanesulfonic acid (HEPES, >99.5%), trimethylchlorosilane (>99%), hydrochloric acid (>36.5-38%), potassium chloride (>99%), and sodium fluorescein (BioReagent, suitable for fluorescence). Polydimethylsiloxane (PDMS, Dow Sylgard 184) was purchased from Ellsworth Adhesives. Silicon wafers (100 mm diameter) were purchased from Silicon Materials. SU-8 3050 photoresist and developer were purchased from MicroChem. Polytetrafluoroethylene (PTFE) tubing (1/16" outer diameter, 250 µm inner diameter) was purchased from Chromatographic Specialties.

Design and fabrication of the microfluidic platform

The microfluidic devices are based on a prior design.[59] They have two layers, one which contains the features required to make droplets (the T-junction) and the other which contains the features required to make DIBs (rail that is used to bring the phospholipid monolayer-covered droplets into contact with each other). Target height for each layer was 50 µm.

Microfluidic devices were fabricated as described previously[8] using traditional photolithography and soft lithography techniques. In brief, features were designed using Auto-

CAD (Autodesk, 2018) and printed onto two acetate masks at 10 µm resolution by CAD/Art Services. To create the mould using photolithography, a layer of photoresist was spin-coated onto a silicon wafer, and baked prior to exposure to UV light (11.2 s, 19.96 mW/cm^2, OAI Model 800 mask aligner) through the first photomask. Then, a second layer was spin-coated onto the first one, soft-baked, and exposed to UV using the second photomask. Unexposed features from both layers were removed with developer and the mould was subjected to a final hard bake (30 min at 200 °C) and a final UV exposure (90 s, 19.96 mW/cm^2).

To fabricate the microfluidic device using soft lithography, PDMS was prepared as directed by the manufacturer (previously described in detail[8]), poured over the mould, degassed to remove air bubbles, and cured overnight at 65°C. The PDMS microfluidic device was then removed from the mould, and access holes were punched using a 1 mm biopsy punch to fit the outer diameter of the tubing that connects the microfluidic device to the pressure pump. To create the base of the device, degassed PDMS was spincoated at 1200 rpm for 25 s onto the surface of glass microscope slides to create a thin layer. Both the PDMS devices and the PDMS-coated glass slides were washed, dried with filtered air, and baked at 90 °C for 30 min. The device and the base were then treated with air plasma (Diener Electronic, Zepto ONE, 37 s, 29 W, 1.75 mbar) and permanently bonded to each other. The microfluidic devices were stored at 65 °C for a minimum of 24 h prior to use.

Preparation of phospholipid solutions

All phospholipids were purchased as stock solutions in chloroform. Solutions of vesicles of each phospholipid (or phospholipid formulation) shown in Figure 3 in buffer at a final concentration of 10 mg/mL were prepared. To do so, chloroform was removed from the stock solutions by placing 400 µL of the 25 mg mL^{-1} chloroform stock solutions in a 10 mL glass roundbottom flask, and subjecting them to a stream of nitrogen gas. To ensure that all chloroform was removed, the phospholipids were then placed under vacuum for 1 h. Each phospholipid or phospholipid formulation was them redissolved in 1 mL of aqueous buffer

(pH 7.59, 10mM HEPES, 140mM KCl), vortexing to ensure complete suspension of the phospholipids in the buffer. To create vesicles, these solutions were frozen and thawed 5 times using liquid nitrogen and warm water, before being extruded 21 times through a 0.1 µm polycarbonate membrane (Avanti Polar Lipids) at room temperature. For fluorescein transport experiments, 100 µM sodium fluorescein was added to the buffer.

Operating parameters of the microfluidic platform

To create droplets and then DIBs on the microfluidic platform, a phospholipid solution and squalene oil were placed in reservoirs (1.5 mL Eppendorf tubes, one each for the phospholipid suspension and the oil, see Figure 1) and two equal lengths of PTFE tubing were used to connect the reservoirs to a pressure pump (OB1 MK3, Elveflow). Squalene and aqueous buffers were introduced into the microfluidic device by applying a pressure of 100 mbar to both reservoirs. Once droplet formation began, the pressure on each reservoir was gradually decreased to 20-50 mbar. Following DIB formation, flow was stopped from both reservoirs using the Elveflow control software. To visualise droplet and DIB formation, devices were mounted in a custom-made heating platform[8] on a Nikon Eclipse Ti2-E inverted microscope. Brightfield images were collected using a Genie Nano C1280 camera (Teledyne Dalsa). The specifications of our custom-made heating platform have been previously described in detail.[8] For permeability experiments, we used a microfluidic device containing two parallel droplet and DIB formation geometries (T-junctions, meandering channels, and rails). In a bulk squalene solution, DIBs were formed between pairs of droplets: a donor droplet containing a 100 µM solution of sodium fluorescein in buffer and an acceptor droplet containing only buffer in a similar way to that shown previously.[8]

Fluorescence data collection

Once a DIB pair formed and the flow was stopped, brightfield and fluorescence images were taken every 5 s with a 10 ms exposure time until experiment termination. DIBs were formed

at the required T_m and the platform temperature was then decreased to 37°C for permeability measurements. Quantification of fluorescence intensity was performed via time-based measurement of mean intensity in regions of interest (ROIs) within each droplet in each frame using NIS Elements. Fluorescence intensity data was normalised for phospholipid bilayer surface area and droplet volume as previously described.[8] Briefly, bilayer diameters and droplet semiaxes were measured using, respectively, the "Distance Measurement" and the "Measurements and Annotations" modules in NIS Elements. Subsequent calculations were performed by approximating artificial cell membrane surface areas as ellipses and droplet volumes as ellipsoids (Figures S2-S5). Each data set in this paper represents 2-5 replicates performed on different microfluidic devices. Different microfluidic devices were used to ensure reproducibility and to remove variables associated with the device itself from the measurements.

DIB formation data collection

Bilayer diameters and droplet semiaxes were measured before, during, and after DIB formation using the "Distance Measurement" and the "Measurements and Annotations" modules in NIS Elements. Subsequent calculations were performed by approximating droplet circumferences as ellipses.

Interfacial tension measurements

Interfacial tension measurements were performed through pendant drop tensiometry using a DataPhysics TBU90E goniometer. A 0.9 mm needle tip was used to dispense a 10 µL droplet of each phospholipid suspension into a cuvette filled with squalene. This was repeated in triplicate for each phospholipid formulation. Eight images were collected of each droplet and analysed in OpenDrop. The density of the phospholipid suspensions was determined to be 0.956 g mL^{-1}. Measured interfacial tension values, half DIB contact angles, and calculated membrane lateral pressures are provided in Table S2.

Contributions

JLK performed the experimental work and data analysis. KSE developed part of the initial device design. JLK and KSE wrote the manuscript.

Acknowledgement

The authors thank the Centre for Advanced Materials and Related Technology (CAMTEC) at the University of Victoria for access to cleanroom facilities. This research was funded through the Natural Sciences and Engineering Research Council of Canada (NSERC) Discovery grant program. Dr Elvira's position is funded through the Canada Research Chair program and through the Michael Smith Foundation of Health Research Scholar program in partnership with the Pacific Alzheimer Research Foundation. Her laboratory was equipped using funding from the Canada Foundation for Innovation John R. Evans Leaders Fund, the British Columbia Knowledge Development Fund (BCKDF) and the NSERC Research Tools and Instruments program. We also thank Elanna Stephenson and Matt Noseworthy for developing the device designs, especially Elanna for developing the two-rail design as shown in our prior publication. Finally, we thank Ned Djilali for use of his goniometer.

References

(1) Mueller, P.; Rudin, D. O.; Ti Tien, H.; Wescott, W. C. Reconstitution of cell membrane structure in vitro and its transformation into an excitable system. *Nature* **1962**, *194*, 979–980.

(2) Bangham, A. D.; Hill, M. W.; Miller, N. G. A. In *Methods in Membrane Biology: Volume 1*; Korn, E. D., Ed.; Springer US: Boston, MA, 1974; pp 1–68.

(3) Carugo, D.; Bottaro, E.; Owen, J.; Stride, E.; Nastruzzi, C. Liposome production by microfluidics: potential and limiting factors. *Scientific Reports* **2016**, *6*, 25876.

(4) Robinson, T. In *Advances in Biomembranes and Lipid Self-Assembly*; Lipowsky, R., Ed.; Multiresponsive behavior of biomembranes and giant vesicles; Academic Press, 2019; Vol. 30; pp 271–315.

(5) Deng, N.-N.; Huck, W. T. S. Microfluidic formation of monodisperse coacervate organelles in liposomes. *Angewandte Chemie International Edition* **2017**, *56*, 9736–9740.

(6) Ugrinic, M.; Zambrano, A.; Berger, S.; Mann, S.; Tang, T.-Y. D.; deMello, A. Microfluidic formation of proteinosomes. *Chemical Communications* **2018**, *54*, 287–290.

(7) Hutter, I.; Müller, E.; Kristiansen, P. M.; Kresak, S.; Tiefenauer, L. Polymer-based microfluidic device for measuring membrane protein activities. *Microfluidics and Nanofluidics* **2013**, *14*, 421–429.

(8) Korner, J. L.; Stephenson, E. B.; Elvira, K. S. A bespoke microfluidic pharmacokinetic compartment model for drug absorption using artificial cell membrane. *Lab on a Chip* **2020**, *20*, 1898–1906.

(9) Funakoshi, K.; Suzuki, H.; Takeuchi, S. Lipid bilayer formation by contacting monolayers in a microfluidic device for membrane protein analysis. *Analytical Chemistry* **2006**, *78*, 8169–8174.

(10) Nisisako, T.; Portonovo, S. A.; Schmidt, J. J. Microfluidic passive permeability assay using nanoliter droplet interface lipid bilayers. *Analyst* **2013**, *138*, 6793–6800.

(11) Braziel, S.; Sullivan, K.; Lee, S. Quantitative Raman microspectroscopy for water permeability parameters at a droplet interface bilayer. *Analyst* **2018**, *143*, 747–755, Publisher: The Royal Society of Chemistry.

(12) Dixit, S. S.; Pincus, A.; Guo, B.; Faris, G. W. Droplet Shape Analysis and Permeability Studies in Droplet Lipid Bilayers. *Langmuir : the ACS journal of surfaces and colloids* **2012**, *28*, 7442–7451.

(13) Hwang, W. L.; Holden, M. A.; White, S.; Bayley, H. Electrical behavior of droplet interface bilayer networks:experimental analysis and modeling. *Journal of the American Chemical Society* **2007**, *129*, 11854–11864.

(14) Creasy, M. A.; Leo, D. J. Non-invasive measurement techniques for measuring properties of droplet interface bilayers. *Smart Materials and Structures* **2010**, *19*, 094016, Publisher: IOP Publishing.

(15) Freeman, E. C.; Najem, J. S.; Sukharev, S.; Philen, M. K.; Leo, D. J. The mechanoelectrical response of droplet interface bilayer membranes. *Soft Matter* **2016**, *12*, 3021–3031, Publisher: The Royal Society of Chemistry.

(16) Stanley, C. E.; Elvira, K. S.; Niu, X. Z.; Gee, A. D.; Ces, O.; Edel, J. B.; Demello, A. J. A microfluidic approach for high-throughput droplet interface bilayer (DIB) formation. *Chemical Communications* **2010**, *46*, 1620–1622.

(17) Hwang, W. L.; Chen, M.; Cronin, B.; Holden, M. A.; Bayley, H. Asymmetric droplet interface bilayers. *Journal of the American Chemical Society* **2008**, *130*, 5878–5879.

(18) Elani, Y.; J. deMello, A.; Niu, X.; Ces, O. Novel technologies for the formation of 2-D and 3-D droplet interface bilayer networks. *Lab on a Chip* **2012**, *12*, 3514–3520.

(19) Punnamaraju, S. Voltage and Photo Induced Effects in Droplet-Interface-Bilayer Lipid Membranes. Ph.D. thesis, University of Cincinnati, 2011.

(20) Malmstadt, N.; Nash, M. A.; Purnell, R. F.; Schmidt, J. J. Automated formation of lipid-bilayer membranes in a microfluidic device. *Nano Letters* **2006**, *6*, 1961–1965.

(21) Holden, M. A.; Needham, D.; Bayley, H. Functional bionetworks from nanoliter water droplets. *Journal of the American Chemical Society* **2007**, *129*, 8650–8655.

(22) Syeda, R.; Holden, M. A.; Hwang, W. L.; Bayley, H. Screening blockers against a potassium channel with a droplet interface bilayer array. *Journal of the American Chemical Society* **2008**, *130*, 15543–15548.

(23) Kara, S.; Afonin, S.; Babii, O.; Tkachenko, A. N.; Komarov, I. V.; Ulrich, A. S. Diphytanoyl lipids as model systems for studying membrane-active peptides. *Biochimica et Biophysica Acta (BBA) - Biomembranes* **2017**, *1859*, 1828–1837.

(24) Faugeras, V.; Duclos, O.; Bazile, D.; Thiam, A. R. Membrane determinants for the passive translocation of analytes through droplet interface bilayers. *Soft Matter* **2020**, *16*, 5970–5980.

(25) Findlay, H. E.; Harris, N. J.; Booth, P. J. In vitro synthesis of a major facilitator transporter for specific active transport across droplet interface bilayers. *Scientific Reports* **2016**, *6*, 1–9.

(26) Barlow, N. E.; Bolognesi, G.; Haylock, S.; Flemming, A. J.; Brooks, N. J.; Barter, L. M. C.; Ces, O. Rheological droplet interface bilayers (rheo-DIBs): probing the unstirred water layer effect on membrane permeability via spinning disk induced shear stress. *Scientific Reports* **2017**, *7*, 1–12.

(27) Taylor, G. J.; Sarles, S. A. Heating-enabled formation of droplet interface bilayers using Escherichia coli total lipid extract. *Langmuir* **2015**, *31*, 325–337.

(28) Barlow, N. E.; Smpokou, E.; Friddin, M. S.; Macey, R.; Gould, I. R.; Turnbull, C.; Flemming, A. J.; Brooks, N. J.; Ces, O.; Barter, L. M. C. Engineering plant membranes using droplet interface bilayers. *Biomicrofluidics* **2017**, *11*.

(29) Taylor, G. J.; Heberle, F. A.; Seinfeld, J. S.; Katsaras, J.; Collier, C. P.; Sarles, S. A. Capacitive detection of low-enthalpy, higher-order phase transitions in synthetic and natural composition lipid membranes. *Langmuir* **2017**, *33*, 10016–10026.

(30) Cooper, G. M. Cell membranes. *The Cell: A Molecular Approach.* **2000**,

(31) Bretscher, M. S.; Raff, M. C. Mammalian plasma membranes. *Nature* **1975**, *258*, 43–49.

(32) van Meer, G.; Voelker, D. R.; Feigenson, G. W. Membrane lipids: where they are and how they behave. *Nature reviews. Molecular cell biology* **2008**, *9*, 112–124.

(33) Brain Extract Total. `https://avantilipids.com/product/131101`.

(34) Najem, J. S.; Taylor, G. J.; Armendarez, N.; Weiss, R. J.; Hasan, M. S.; Rose, G. S.; Schuman, C. D.; Belianinov, A.; Sarles, S. A.; Collier, C. P. Assembly and Characterization of Biomolecular Memristors Consisting of Ion Channel-doped Lipid Membranes. *Journal of Visualized Experiments: JoVE* **2019**,

(35) Najem, J. S.; Taylor, G. J.; Weiss, R. J.; Hasan, M. S.; Rose, G.; Schuman, C. D.; Belianinov, A.; Collier, C. P.; Sarles, S. A. Memristive Ion Channel-Doped Biomembranes as Synaptic Mimics. *ACS Nano* **2018**, *12*, 4702–4711, Publisher: American Chemical Society.

(36) Yanagisawa, M.; Yoshida, T.-a.; Furuta, M.; Nakata, S.; Tokita, M. Adhesive force between paired microdroplets coated with lipid monolayers. *Soft Matter* **2013**, *9*, 5891–5897, Publisher: The Royal Society of Chemistry.

(37) Ringley, J. D.; Sarles, S. A. Temperature-Controlled Assembly and Characterization of a Droplet Interface Bilayer. *Journal of Visualized Experiments: JoVE* **2021**,

(38) Lee, S.; Kim, D. H.; Needham, D. Equilibrium and Dynamic Interfacial Tension Measurements at Microscopic Interfaces Using a Micropipet Technique. 1. A New Method

for Determination of Interfacial Tension. *Langmuir* **2001**, *17*, 5537–5543, Publisher: American Chemical Society.

(39) Schlicht, B.; Zagnoni, M. Droplet-interface-bilayer assays in microfluidic passive networks. *Scientific Reports* **2015**, *5*, 9951.

(40) Casadevall i Solvas, X.; deMello, A. Droplet microfluidics: recent developments and future applications. *Chemical Communications* **2011**, *47*, 1936–1942.

(41) Debon, A. P.; Wootton, R. C. R.; Elvira, K. S. Droplet confinement and leakage: Causes, underlying effects, and amelioration strategies. *Biomicrofluidics* **2015**, *9*.

(42) Venkatesan, G. A.; Lee, J.; Farimani, A. B.; Heiranian, M.; Collier, C. P.; Aluru, N. R.; Sarles, S. A. Adsorption Kinetics Dictate Monolayer Self-Assembly for Both Lipid-In and Lipid-Out Approaches to Droplet Interface Bilayer Formation. *Langmuir* **2015**, *31*, 12883–12893, Publisher: American Chemical Society.

(43) Abbyad, P.; Dangla, R.; Alexandrou, A.; Baroud, C. N. Rails and anchors: guiding and trapping droplet microreactors in two dimensions. *Lab on a Chip* **2011**, *11*, 813–821.

(44) Niu, X.; Gulati, S.; Edel, J. B.; deMello, A. J. Pillar-induced droplet merging in microfluidic circuits. *Lab on a Chip* **2008**, *8*, 1837–1841, Publisher: The Royal Society of Chemistry.

(45) Antonietti, M.; Förster, S. Vesicles and liposomes: a self-assembly principle beyond lipids. *Advanced Materials* **2003**, *15*, 1323–1333.

(46) Boggs, J. M. Lipid intermolecular hydrogen bonding: influence on structural organization and membrane function. *Biochimica et Biophysica Acta (BBA) - Reviews on Biomembranes* **1987**, *906*, 353–404, Publisher: Elsevier.

(47) Proulx, P. Structure-function relationships in intestinal brush border membranes.

Biochimica et Biophysica Acta (BBA) - Reviews on Biomembranes **1991**, *1071*, 255–271.

(48) Sugano, K.; Hamada, H.; Machida, M.; Ushio, H.; Saitoh, K.; Terada, K. Optimized conditions of bio-mimetic artificial membrane permeation assay. *International Journal of Pharmaceutics* **2001**, *228*, 181–188.

(49) Liver PC. `https://avantilipids.com/product/840055`, Library Catalog: avantilipids.com.

(50) Phase transition temperatures for glycerophospholipids. `https://avantilipids.com/tech-support/physical-properties/phase-transition-temps`, Library Catalog: avantilipids.com.

(51) McMahon, H. T.; Boucrot, E. Membrane curvature at a glance. *J Cell Sci* **2015**, *128*, 1065–1070.

(52) Furse, S.; Brooks, N. J.; Seddon, A. M.; Woscholski, R.; Templer, R. H.; Tate, E. W.; Gaffney, P. R. J.; Ces, O. Lipid membrane curvature induced by distearoyl phosphatidylinositol 4-phosphate. *Soft Matter* **2012**, *8*, 3090–3093, Publisher: The Royal Society of Chemistry.

(53) Shearman, G. C.; Ces, O.; Templer, R. H.; Seddon, J. M. Inverse lyotropic phases of lipids and membrane curvature. *Journal of Physics. Condensed Matter: An Institute of Physics Journal* **2006**, *18*, S1105–1124.

(54) Janmey, P. A.; Kinnunen, P. K. J. Biophysical properties of lipids and dynamic membranes. *Trends in Cell Biology* **2006**, *16*, 538–546, Publisher: Elsevier.

(55) Bayley, H.; Cronin, B.; Heron, A.; Holden, M. A.; Hwang, W.; Syeda, R.; Thompson, J.; Wallace, M. Droplet interface bilayers. *Molecular bioSystems* **2008**, *4*, 1191–1208.

(56) Beltramo, P. J.; Scheidegger, L.; Vermant, J. Toward Realistic Large-Area Cell Membrane Mimics: Excluding Oil, Controlling Composition, and Including Ion Channels. *Langmuir* **2018**, *34*, 5880–5888, Publisher: American Chemical Society.

(57) Huang, Y.; Chandran Suja, V.; Tajuelo, J.; Fuller, G. G. Surface energy and separation mechanics of droplet interface phospholipid bilayers. *Journal of The Royal Society Interface* **2021**, *18*, 20200860, Publisher: Royal Society.

(58) Boreyko, J. B.; Polizos, G.; Datskos, P. G.; Sarles, S. A.; Collier, C. P. Air-stable droplet interface bilayers on oil-infused surfaces. *Proceedings of the National Academy of Sciences* **2014**, *111*, 7588–7593, Publisher: National Academy of Sciences Section: Biological Sciences.

(59) Carreras, P.; Elani, Y.; Law, R. V.; Brooks, N. J.; Seddon, J. M.; Ces, O. A microfluidic platform for size-dependent generation of droplet interface bilayer networks on rails. *Biomicrofluidics* **2015**, *9*, 064121.